Turkish Journal of Civil Engineering, 2023 173-195, Paper 730, ***Research Article***

Strengthening System Effects on the Out-Of-Plane Mechanisms Activation of Masonry Walls under Tsunami Loads

Stefano BELLIAZZI[1]
Gian Piero LIGNOLA[2]
Andrea PROTA[3]

ABSTRACT

The vulnerability of masonry structures against tsunami loads is a highly debated topic in the research community due to the impact in the risk evaluation. The main aim of this paper is to examine the structural response of masonry walls against tsunami loads in terms of out-of-plane local mechanism activation. Furthermore, a critical discussion is proposed about the influence of strengthening system parameters on the out-of-plane response of the masonry wall. Results of parametric analyses are shown in dimensionless form to analyse the effects of main parameters, both for masonry walls and tsunami waves, on the structural response. The analyses results are the bases to design strengthening systems with fiber-reinforced composite materials in order to reduce the vulnerability of masonry structures under tsunami loads.

Keywords: Tsunami, masonry structures, strengthening systems.

1. INTRODUCTION

Tsunami risk assessment ([1], [2], [3]) has become an important research theme due to the high reconstruction costs and human casualties associated with the events of the last decades, such as the 2004 Great Indian Ocean Tsunami [4], the 2010 Chile Tsunami [5], and the 2011 Great East Japan Tsunami [6]. A tsunami is a complex phenomenon based on the wave propagation theory; it can be triggered by several different phenomena including earthquakes

Note:
- This paper was received on August 25, 2022 and accepted for publication by the Editorial Board on January 27, 2023.
- Discussions on this paper will be accepted by May 31, 2023.
- https://doi.org/10.18400/tjce.1247194

1 University of Naples "Federico II", Department of Structures, Napoli, Italy
stefano.belliazzi@unina.it - https://orcid.org/0000-0002-0471-3601

2 University of Naples "Federico II", Department of Structures, Napoli, Italy
glignola@unina.it - https://orcid.org/0000-0001-6027-9291

3 University of Naples "Federico II", Department of Structures, Napoli, Italy
andrea.prota@unina.it - https://orcid.org/0000-0003-3820-663X

or submarine landslides. To assess the tsunami risk of a specific area, a multi-hazard approach should be considered to capture complex scenarios.

A key component in tsunami risk assessment [7] is the vulnerability assessment of buildings under tsunami loads. International building codes, standards, and guidelines provide different approaches to design tsunami-resistant structures.

The ASCE 7-22 [8] proposes an advanced approach to analyse several effects of the tsunami wave impact on the structures; impact of debris, horizontal and vertical load components are modelled on the structure. Furthermore, several coefficients are defined to analyse the effects of the wave direction on the structures. The wave parameters (e.g. inundation depth, wave velocity, moment of flux) are evaluated by the Energy Grade Line analysis where the tsunami flux is modelled as a unidirectional flow.

However, simplified models are available, too, as the Japanese guideline proposal [9] where the tsunami effects on the structure are modelled by an equivalent hydrostatic load distribution. In this model, the expected inundation depth is amplified in order to indirectly analyse the hydrodynamic effects. The Japanese guidelines are based on previous research activities conducted by Asakura et al. [10] and Okada et al. [11].

Furthermore, tsunami wave effects on structures have been analysed by an experimental program with scaled specimens [12] in order to retrieve empirical equations.

The vulnerability of structures under tsunami loads is completely different from the seismic load due to the different type of loads. In fact, seismic forces arise from inertia effects that excite the entire structure, while tsunami loads are predominantly characterized by surface forces over the inundated elements. As a result, the behaviour of buildings under tsunami loading differs from the response to seismic actions. However, both types of loads will have a combined effect on the gravity and lateral force resisting systems for the components at or below the inundation level. In addition, the modelling of tsunami effects on buildings is characterized by a high degree of uncertainty due to wave parameters and topographic information required to quantify tsunami loads [11].

In literature, the available reports on behaviour of masonry structures after a tsunami event show a high vulnerability of masonry structures to tsunami loads; the main collapse mechanisms are related to geotechnical failure (e.g. liquefaction) or local mechanisms activation (e.g. out-of-plane local mechanisms) ([13], [14]).

Preliminary mechanical analyses and studies focalize the attention on the local-mechanisms activation for both in-plane (IP) and out-of-plane (OOP) mechanisms [15] due to the high stresses at the ground floor [16] in terms of bending moment and shear. The vulnerability of the masonry structures is highly influenced by the geometrical characteristics of the masonry wall in terms of wall length and wall thickness [17].

The vulnerability assessment is the main step to develop risk mitigation techniques like as strengthening of strategic structures ([18], [19]), early warning systems or evacuation buildings.

2. RESEARCH SIGNIFICANCE

The goal of this paper is to analyse the vulnerability of masonry walls under tsunami loads in terms of out-of-plane local mechanisms activation.

Belliazzi et al. [20] analysed the effects of the strengthening systems with composite material (e.g. Fiber Reinforced Polymer, FRP, or Fiber Reinforced Cementitious Matrix, FRCM) in tension on the vulnerability of masonry walls under tsunami loads and preliminary results were provided assuming a simplified model for the tsunami loads.

The aim of this work is to improve the basis of the previous analyses [20] assuming a more refined model for the tsunami loads. Equations in dimensionless form are proposed to provide results applicable to any masonry cross-section. However, it is worth noting that masonry suffering for premature disaggregation (e.g. stone masonry walls made of weak mortar, irregular small blocks, and non-connected wall leaves) is not able to develop local mechanisms [21], hence are out of the present investigation.

In addition, parametric analyses have been performed to analyse the effects of the main parameters and coefficients of the proposed equation.

The overall results of these analyses allow to increase confidence on the design of strengthening systems with fiber-reinforced composite materials in tension in order to reduce the vulnerability of masonry structures under tsunami loads.

3. TSUNAMI LOAD MODEL

In the current literature, several approaches are available to model tsunami inundation forces on buildings due to the high degree of uncertainties in the fluid mechanics modelling.

The ASCE 7-22 proposes an advanced model where hydrostatic and hydrodynamic effects are defined separately and several parameters are required to model the tsunami forces. The Japanese guidelines propose a conservative approach where the tsunami loads are modelled by one equivalent hydrostatic distribution and the expected inundation depth is amplified in order to consider the hydrodynamic effects.

Therefore, the ASCE 7-22 requires a high knowledge of the structure and of the wave characteristics. The Japanese guideline is easier to use than the ASCE 7-22, but the tsunami force on the structure is usually overestimated. It is clear that the Japanese approach is recommended if a low knowledge level is achievable, e.g. in large-scale analysis [22].

In this paper, Foster et al. [12] approach is assumed to describe the tsunami inundation forces on the structure. The method allows to consider hydrostatic and hydrodynamic loads depending on the inundation depth and the flow velocity. In particular, the flow velocity depends on the Froud number, Fr (a dimensionless value that describes different flow regimes). An empirically equation for hydrodynamic loads is provided, dependent upon the Froude number of the flow and blocking fraction (the ratio between the structure width and the flow width), based on experimental results [12]. In the experimental activity, the water waves were generated by a tsunami simulator and the structures have been realized by means of scaled specimens.

Therefore, the equation for the hydrostatic load (Eq. 1 - F_s represents the resultant of the hydrostatic load distribution) is related to a linear distribution while the equations for the hydrodynamic load (Eq. 2 and Eq. 3 - F_d represent the resultant of the hydrodynamic load distribution) are related to a uniform distribution depending on the flow regime.

$$F_s = 0.5 \cdot \rho_s \cdot g \cdot L \cdot h^2 \quad (1)$$

If $F_r < 1$ (subcritical regime):

$$F_d = 0.5 \cdot C_D \cdot \rho_s \cdot L \cdot u^2 \cdot h \quad (2)$$

If $F_r \geq 1$ (choked regime):

$$F_d = \lambda \cdot \rho_s \cdot L \cdot \sqrt[3]{g} \cdot \sqrt[3]{(u \cdot h)^4} \quad (3)$$

Where ρ_s is the flow density, g is the gravitational acceleration constant, h is the expected inundation depth, u is the flow velocity, L is the wall length exposed to the tsunami wave, C_D is the drag coefficient and λ is an empirical coefficient.

$$C_D = 1.9 \cdot (1 + 1.9 \cdot (b/w)/2)^2 \quad (4)$$

$$\lambda = 0.73 + 1.2 \cdot (b/w) + 1.1 \cdot (b/w)^2 \quad (5)$$

Where b is the width of the structure, w is the channel width and the ratio b/w is named blocking fraction [23]. The blocking fraction generates high instability in hydraulic calculation: higher blocking fractions increase the tendency of the flow regime to change from subcritical to choked [24].

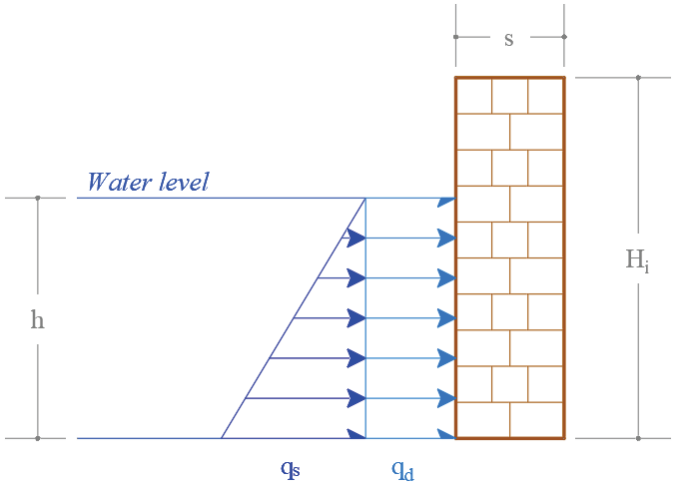

Figure 1 - Tsunami inundation forces model (s is the wall thickness, H_i is the interstorey height, q_s is the maximum hydrostatic load, q_d is the uniform hydrodynamic load)

The flow velocity u and the Froude number F_r are dependent on Eq. 6.

$$u = \frac{F_r}{\sqrt{g \cdot h}} \tag{6}$$

In addition, an opening ratio coefficient α is assumed (variable between 0.7 and 1) to consider the effects of the wall openings, according to ASCE 7-22 [8]. The wall opening coefficient is defined as one minus the ratio between the openings area and the gross wall area.

The structure is loaded by a trapezoidal load pattern equal to the sum of the hydrostatic and the hydrodynamic components (Figure 1).

4. MATERIAL CONSTITUTIVE MODEL

Several stress-strain relationships are proposed in international codes and guidelines to model the non-linear mechanical response of masonry and strengthening systems.

Different failure modes could be reached as masonry crushing or strengthening system failure in tension depending on material properties combination.

The compressive behaviour of masonry is modelled by rectangular stress-block model (Figure 2.a) according to Eurocode 6 [25]. The stress-block model is characterized by effective height ψ, effective depth of compression zone centre λ_m and the compressive strength f_m. ψ and λ_m are equal to 0.8 and 0.4, respectively, based on parabolic-rectangular stress strain relationship assuming the end of parabola at strain ε_{m0} equal to 2‰ and ultimate strain ε_{mu} equal to 3.5‰ according to Eurocode 6 [25]. These stress-block parameters are reasonable if the masonry crushing failure mode is reached.

The stress-block model is assumed as constitutive model in compression of masonry due to simplification in the calculation in order to retrieve equations in dimensionless form coherently with the goal of the paper.

Strengthening system behaviour in tension and failure modes are influenced by combination of matrix and fibers in terms of individual material properties and thicknesses. Main experimental programs show that the mechanical behaviour in tension is approximated by linear, bilinear or trilinear behaviour [26].

Furthermore, the fibers have a linear behaviour while the inorganic matrix influences the response at low strain values with its tension stiffening. In the following cross-section analysis, a linear tensile behaviour (Figure 2.b) is assumed in tension for composite strengthening systems with organic matrix (e.g. FRP) according to Italian guideline CNR-DT 200R1/2013 [27] or due to the assumptions that the inorganic matrix (e.g. FRCM) is cracked as shown in Italian guideline CNR-DT 215/2018 [28]. In particular, the linear behaviour is defined by ultimate tensile strength f_{fu}, an elastic modulus E_f and an ultimate strengthening system strain ε_{fu}, either due to fiber rupture or debonding failure ([26], [29]).

The compressive behaviour of composite strengthening systems is neglected according to Italian guidelines CNR-DT 200 R1/2013 [27] and CNR DT 215/2018 [28].

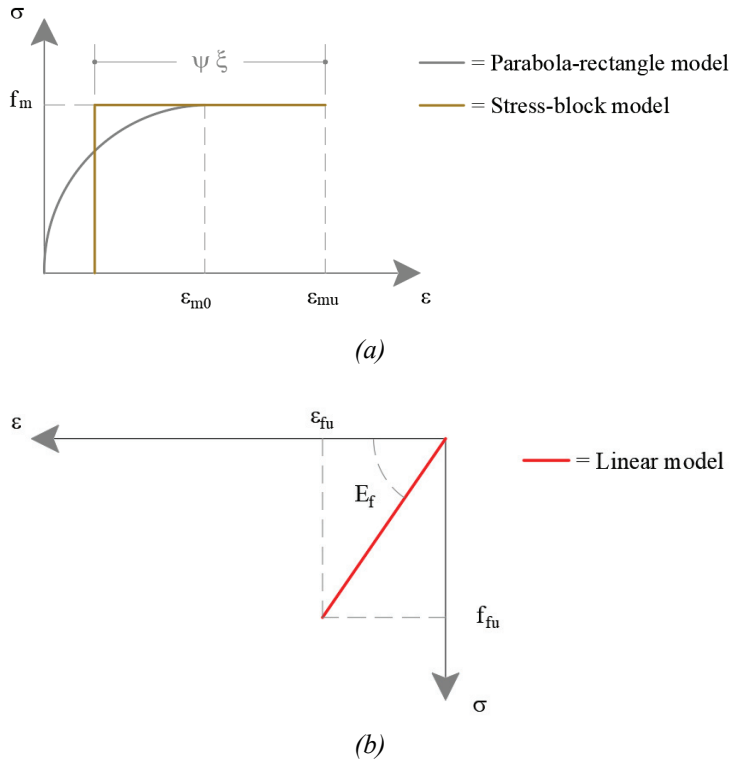

Figure 2 - Constitutive model of masonry in compression (a) and strengthening system in traction (b)

5. CROSS-SECTION ANALYSIS

Cross-section analysis is performed in order to analyse the activation of OOP local mechanisms and the effects of the strengthening system on the flexural capacity.

The cross-section analysis is performed at the ultimate limit state considering the following basic assumptions according to Italian CNR guidelines (CNR-DT 200R1/2013 [27] and CNR-DT 215/2018 [28]):

- Conservation of plain sections allow to assume linear strain diagrams, also known as the Bernoulli-Navier assumption;
- The shear deformability is neglected according to the Bernoulli assumption;
- Tensile behaviour of masonry is negligible;
- Strengthening system is effective only in traction and never in compression due to composite slenderness, as basic assumption;
- Perfect bond between strengthening system and masonry that allows to consider strengthening system strain ε_f equal to surrounding masonry strain ε_m (Eq. 7) without slip phenomena;

- The ultimate condition of the cross-section is related to compressed masonry crushing or tensile failure of the composite system depending on composite mechanical characteristics as shown in the following.

$$\varepsilon_m = \varepsilon_f \tag{7}$$

The proposed dimensionless equations are based on equilibrium equations [30] (Figure 3).

The axial forces are divided by the cross-section width, b_m, the cross-section height, s, and the compressive strength, f_m, while the bending moment is divided by $b_m\, s^2\, f_m$.

The dimensionless bending capacity equation $m_{R,0}$ (Eq. 9) of the unreinforced masonry structure (URM) cross-section is easily retrieved in the case of cross-section without strengthening system. It depends on the dimensionless external vertical axial load, n_0, (Eq. 8), the wall thickness, s, and the interstorey height, H_i; in particular, the ratio between the wall thickness s and the interstorey height H_i represents the geometrical vertical slenderness, H_i/s, of the masonry wall.

$$n_0 = 0.8 \cdot \xi \tag{8}$$

$$m_{R,0} = 0.5 \cdot n_0 \cdot \frac{s}{H_i} \cdot (1 - n_0) \tag{9}$$

Where ξ represents the dimensionless neutral axis depth; the neutral axis, x, is divided by the cross-section height, s.

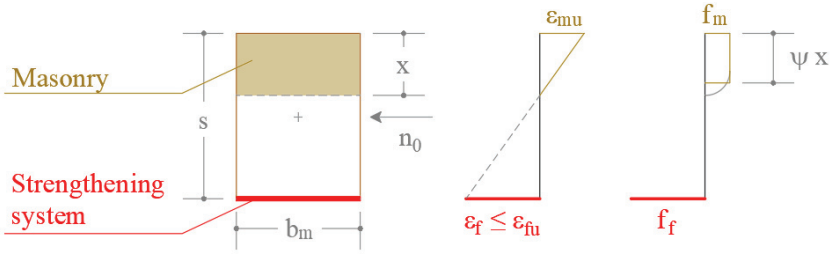

Figure 3 - Cross-section model

In the case of strengthening system applied to masonry cross-section, the dimensionless bending capacity equation $m_{R,\omega}$ (Eq. 11) is retrieved by a rotational equilibrium between the compressive masonry resultant and the tensile strengthening system resultant and it depends on the dimensionless external axial load, n_ω, (Eq. 10), the geometrical vertical slenderness, H_i/s, of the wall and the composite mechanical ratio, ω.

$$n_\omega = 0.8 \cdot \xi - \frac{1-\xi}{\xi} \cdot \omega \tag{10}$$

$$m_{R,\omega} = 0.4 \cdot \xi \cdot \frac{s}{H_i} \cdot (1 - 0.8\,\xi) + \frac{0.8 - n_\omega}{n_\omega} \cdot \frac{\omega}{2} \cdot \frac{s}{H_i} \quad (11)$$

It is worth noting that the external axial loads n_0 and n_ω depend on the wall self-weight and the effect of upper storeys.

The composite mechanical coefficient, ω, (Eq. 13) is function of different masonry and strengthening system properties according to the dimensionless approach; furthermore, a ratio between the elastic moduli of the two materials can be detected if it is assumed that the elastic modulus of masonry E_m depends on f_m (Eq. 12) [31] according to Eurocode 6 [25] definition.

$$E_m = 10^3 \cdot f_m \quad (12)$$

$$\omega = \frac{t_f}{s} \cdot \frac{\varepsilon_{mu}}{f_m} \cdot E_f = 10^3 \cdot \frac{t_f}{s} \cdot \frac{E_f}{E_m} \cdot \varepsilon_{mu} \quad (13)$$

Where t_f represents the fiber equivalent dry thickness.

The composite mechanical ratio ω allows to define the strengthening system with respect to wall composition in terms of both geometrical and mechanical properties.

6. OUT-OF-PLANE LOCAL MECHANISM

The local mechanism activation is a key aspect of the vulnerability of masonry structures. It depends on several factors as the material properties, the geometry of the wall, the boundary conditions and the connections between structural elements.

Several numerical methods have been employed to assess the OOP behaviour of URM structures. Finite element macro-modelling approaches are the most famous methods to analyse the OOP mechanisms activation even though the high degree of uncertainties may provide a non-realistic result in terms of crack pattern. Another criterion is to discretize the masonry wall in rigid blocks; D'Ayala and Speranza [32] proposed several configurations.

The main OOP local mechanisms are the vertical and the horizontal [27], [33] bending mechanisms (Figure 4), while shear mechanism are usually negligible with commonly slender walls (i.e. high H_i/s ratio). The horizontal bending mechanisms are activated when the external load exceeds the capacity of the cross-section in terms of axial load ([34]). The masonry wall thrust of the internal arch mechanism equilibrates the external load. In this paper, the horizontal bending mechanism [35] is not analysed because it requires a masonry wall without openings for the internal arch mechanism development. Vertical bending mechanism is typical in masonry walls with openings (common for structures in front of the seaside).

The strengthening configuration is based on main fibers applied along the vertical direction over the internal side of the walls (tensile side) with fibers anchored at least at the bottom of the structure. Typical composite mechanical ratio values, mechanical properties, materials, application schemes and few photographs are available in many references and a valuable outline is provided in both Italian CNR guidelines (CNR-DT 200R1/2013 [27] and CNR-DT 215/2018 [28]).

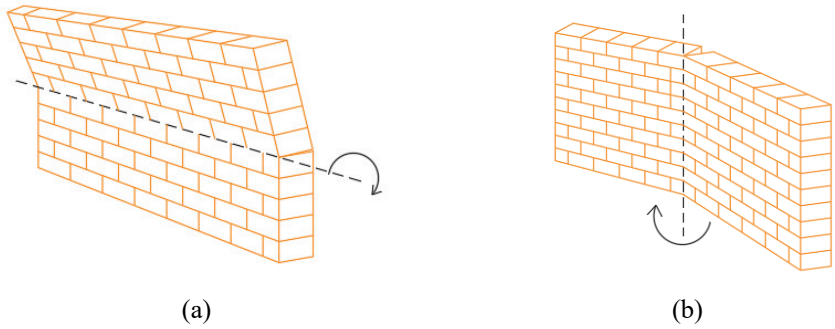

Figure 4 - Vertical (a) and horizontal (b) bending mechanisms

Therefore, the vertical bending [36] OOP mechanism activation is reached when the cross-section capacity is equal to the maximum external load in terms of bending moment.

Linear analyses are performed considering a simply supported beam with a trapezoidal load pattern changing the inundation depth and the Froude number; the Froude number changes in the range between 0.7 and 2.0 [37]. The simply supported beam length is equal to the interstorey height, H_i.

A concentrated external axial load, n, is considered on the top for modelling the wall self-weight and the effect of upper storeys. Therefore, a normalized external axial load on the cross-section is considered, variable in a range from zero up to about 35% of the ultimate axial load capacity of the masonry walls. As it will be seen later, this is an upper axial load threshold, beyond which, the effects of strengthening are negligible [30].

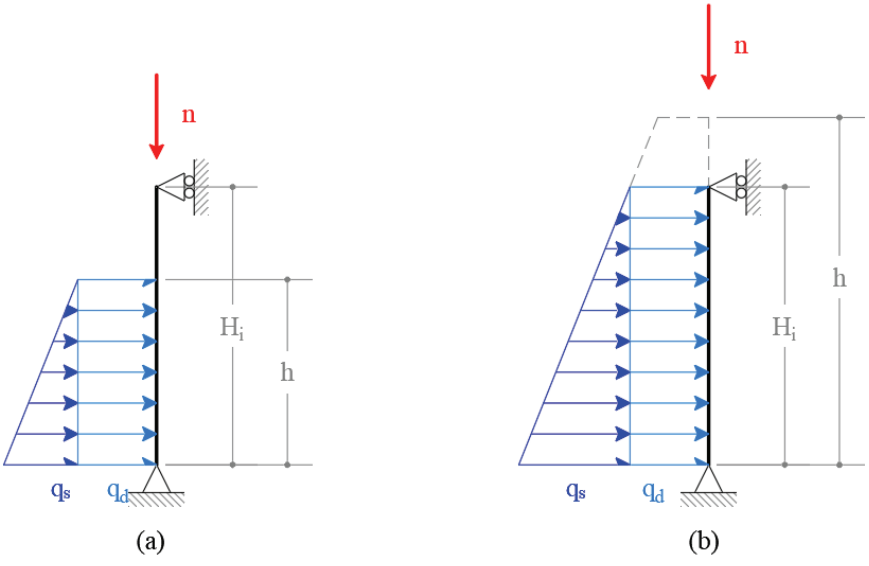

Figure 5 - Static model for $h < H_i$ (a) and $h \geq H_i$ (a)

The maximum bending moment function is simple to derive, considering the static model shown in Figures 5a and 5b.

The masonry wall is loaded with a hydrostatic load q_s and a hydrodynamic load q_d according to Foster et al. [12]:

$$q_s = \gamma_w \cdot L \cdot h \cdot \alpha \tag{14}$$

$$q_d = \beta \cdot \gamma_w \cdot L \cdot h \cdot \alpha \tag{15}$$

Where γ_w is the specific weight of the water, while β is a coefficient depending on the Froud number, if the flow regime is a subcritical regime or chocked regime:

$$\gamma_w = \rho_s \cdot g \tag{16}$$

$$\text{if } F_r < 1, \quad \beta = 0.5 \cdot C_d \cdot F_r^2 \tag{17}$$

$$\text{if } F_r \geq 1, \quad \beta = \lambda \cdot F_r^{4/3} \tag{18}$$

Therefore, equations in dimensionless form of the maximum bending moment are derived depending on the ratio between the inundation depth and the interstorey height.

If $h/H_i < 1$:

$$m_{s,1} = k_1 \cdot \left(\frac{h}{H_i}\right)^3 \cdot [-3 \cdot (\alpha + \beta) + k_2] \cdot \begin{bmatrix} 2 \cdot \frac{h}{H_i} \cdot \alpha \cdot (\alpha + 3\,\beta) + \\ + 3 \cdot (\beta^2 - 2\,\beta\,\alpha - \alpha^2) - (\alpha + \beta) \cdot k_2 \end{bmatrix} \tag{19}$$

If $h/H_i \geq 1$:

$$m_{s,2} = -k_1 \cdot k_3 \left\{-2 \cdot \alpha^2 + 6 \cdot \frac{h}{H_i} \cdot \alpha \cdot (\alpha + \beta) + (\alpha + \beta) \cdot \frac{h}{H_i} \cdot k_3\right\} \tag{20}$$

Where four numerical coefficients k_1, k_2, k_3 and k are defined to simplify the Eqs. 19 and 20:

$$k_1 = \frac{1}{54 \cdot \alpha^2} \cdot k \cdot \left(\frac{H_i}{s}\right)^2 \tag{21}$$

$$k_2 = \sqrt{9 \cdot \beta^2 + 3 \cdot \frac{h}{H_i} \cdot \alpha \cdot (\alpha + 3\,\beta)} \tag{22}$$

$$k_3 = \left[-3 \cdot \frac{h}{H_i} \cdot (\alpha + \beta) + \sqrt{3 \cdot \alpha^2 - 9 \cdot \frac{h}{H_i} \cdot \alpha \cdot (\alpha + \beta) + 9 \cdot \left(\frac{h}{H_i}\right)^2 \cdot (\alpha + \beta)^2}\right] \tag{23}$$

$$k = \frac{\gamma_w \cdot H_i}{f_m} \tag{24}$$

7. PARAMETRIC ANALYSES

Several parametric analyses have been performed to analyse the sensibility of the main parameters of the dimensionless equations.

The tsunami loads depend on the expected inundation depth h and Froude number Fr. Therefore, 3D charts are plotted using Mathworks Matlab where on the x-axis and y-axis are shown the inundation depth h/H_i (in dimensionless form) and the Froude number F_r while on the z-axis is shown the dimensionless bending moment, m_s.

The investigated main parameters are: the external axial load, n, the blocking fraction, b/w, the drag coefficient, C_D, the empirical coefficient, λ, the wall openings coefficient, α, the vertical geometrical slenderness of the wall, H_i/s, the composite mechanical percentage, ω, and the k numerical coefficient.

Each parameter changes in specific range as shown in Table 1 and Table 2. The blocking fraction is assumed equal to 0.1 and 0.6, as representative of different flow regimes [12], [23], [24]. The empirical parameter λ and the drag coefficient C_D are evaluated depending on the blocking fraction coefficient (Table 1). Masonry wall parameters in Table 2 are usual values for masonry buildings in front of the seaside (e.g. in Italy [22]).

The composite mechanical percentage ω is assumed equal to 0.00, 0.01, 0.02, 0.03, and 0.04 in order to consider the URM cross-section and the effects of the strengthening system on the cross-section capacity in terms of ultimate bending moment.

The external axial load n changes among 0.05, 0.15, 0.20, and 0.35.

Table 1 - Wave parameters evaluated depending on blocking fraction b/w

b/w	λ	C_D
0.1	0.86	2.28
0.6	1.85	4.68

Table 2 - Min, mean and max values of the vertical geometrical slenderness of the wall H_i/s, the wall openings coefficient α and the k numerical coefficient

Parameter	Min	Mean	max
H_i/s	2.50	9.58	16.67
α	0.70	0.85	1.00
k	0.003	0.029	0.055

In Figure 6, the effects of the blocking fraction b/w parameter are shown for n equal to 0.05 while the values assumed for the main parameters are shown Table 3. In addition, the representation of the effects of the blocking fraction b/w parameter and of the composite mechanical percentage ω in one figure allow to analyse the combined influence in terms of

external loads (depending on b/w) and cross-section capacity (plane horizontal surfaces depending on ω), respectively.

It is worth noting that at the Froud number value of one, a discontinuity on the maximum bending moment surface is shown due to the abrupt change of the flow regime.

In addition, it is possible to appreciate the effects of the strengthening system on the masonry wall changing the composite mechanical ratio ω. The bending moment capacity of the cross-section does not depend on the inundation depth and the Froude number; therefore, a horizontal plane represents the bending moment capacity.

The scale of the chart does not allow to appreciate the effects of the strengthening systems on the masonry cross-section due to the high values of the external bending moment while increasing the inundation depth (h/H_i); capacity is clearly lower than demand at $h/H_i>0.5$. The dimensionless inundation depth h/H_i allows to clearly define the shift between Eq. 19 or Eq. 20.

Table 3 - Values of the parameters assumed to describe the maximum bending moment surfaces in Figure 6

Parameter	Maximum bending moment - Surface 1	Maximum bending moment - Surface 2
b/w	0.1	0.6
C_D	2.28	4.68
λ	0.86	1.85
α	0.7	0.7
k	0.029	0.029
H_i/s	9.58	9.58

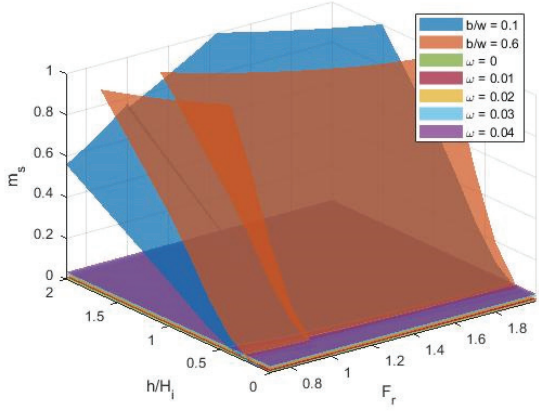

Figure 6 - Effects of the blocking fraction b/w parameter with n = 0.05

Therefore, in Figure 7, the effects of the blocking fraction b/w parameter are shown, for n equal to 0.05, 0.15, 0.20 and 0.35, with a reduced scale in order to understand the effects of the strengthening system and to analyse reasonable values of the external bending moment.

The 3D charts are shown for several external axial load values to investigate the strengthening system effects; in fact, the ultimate bending moment of the cross-section depends on the external axial load parameter while the external bending moment is not affected.

Increasing the external axial load, the effects of the strengthening systems are minimal due to the increase of the neutral axis depth and consequentially, due to the lower strain of the composite. Low composite mechanical values provide yet huge percentage effects in terms of bending moment capacity due to tensile behaviour added to URM cross-section.

For values of the external axial load n higher than 0.05, the composite mechanical ratio ω is limited only to 0.02 and 0.04 because the plan surfaces are almost overlapped.

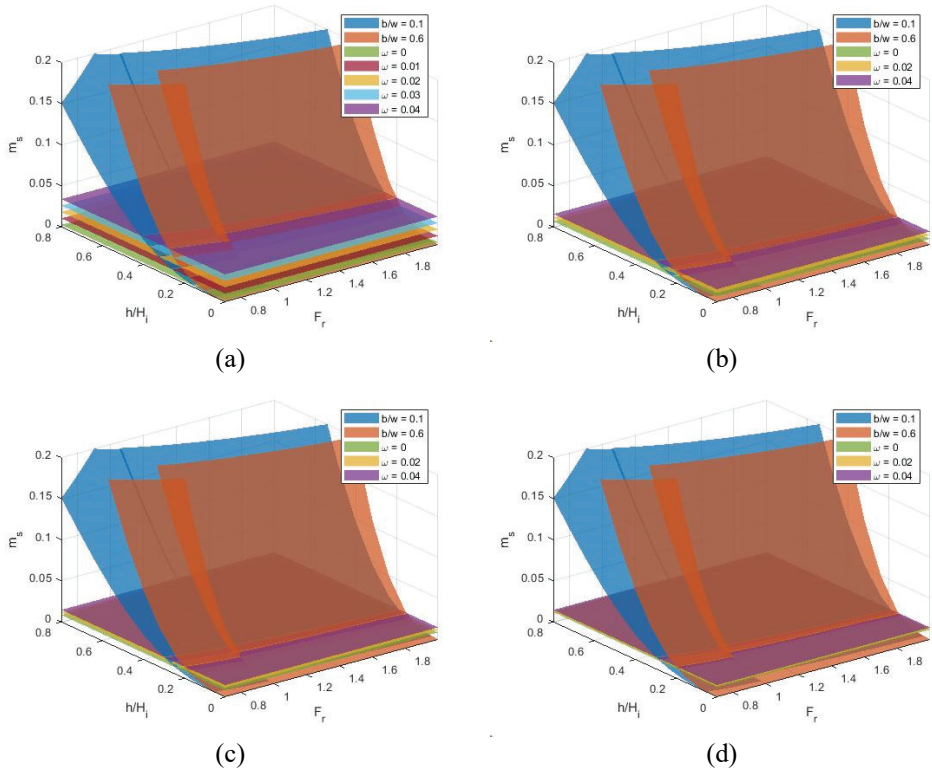

Figure 7 - Effects of the blocking fraction b/w parameter for n equal to 0.05 (a), 0.15 (b), 0.20 (c) and 0.35 (d)

The strengthening system effects become negligible for external load n value higher than 0.35. A masonry wall with higher external axial loads requires other types of strengthening

strategy as the composite reinforced mortar (CRM) ([38], [39]) in order to carry high compression loads, too.

The blocking fraction b/w has high effects on the structural response and it is strictly related to the flow regime. In particular, the vulnerability of the masonry wall increases with the b/w coefficient.

In Figure 8, the effects of the wall openings α parameter are investigated and the values assumed for the main parameters are shown in Table 4.

Table 4 - Values of the parameters assumed to describe the maximum bending moment surfaces in Figure 8

Parameter	Maximum bending moment - Surface 1	Maximum bending moment - Surface 2
b/w	0.1	0.1
C_D	2.28	2.28
λ	0.86	0.86
α	0.7	1
k	0.029	0.029
H_i/s	9.58	9.58

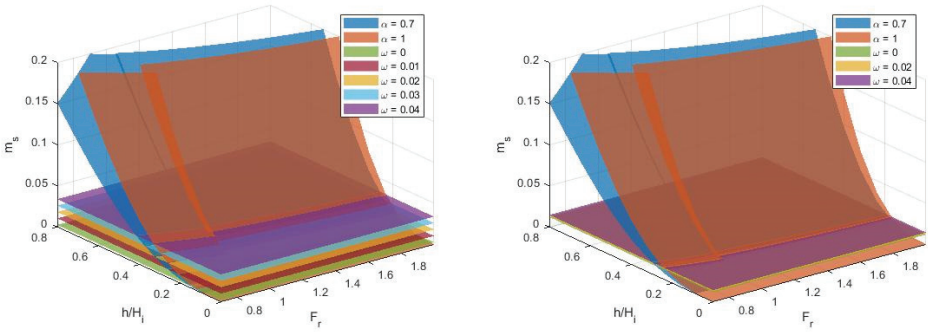

(a) (b)

Figure 8 - Effects of the wall openings α parameter for n equal to 0.05 (a), 0.35 (b)

As expected, the wall openings have a high influence on the vulnerability of masonry wall for several reasons. In fact, the openings reduce the load bearing area of the wall and consequentially, the tsunami forces, hence the influence is in terms of external loads.

In Figure 9, the effects of the geometrical vertical slenderness H_i/s parameter are investigated and the values assumed for the main parameters are shown in Table 5. The strengthening

system effects (different capacity horizontal planes) in terms of composite mechanical ratio ω are not plotted here to focus on H_i/s.

Table 5 - Values of the parameters assumed to describe the maximum bending moment surfaces in Figure 9

Parameter	Maximum bending moment - Surface 1	Maximum bending moment - Surface 2	Maximum bending moment - Surface 3
b/w	0.1 - 0.6	0.1 - 0.6	0.1 - 0.6
C_D	2.28 - 4.68	2.28 - 4.68	2.28 - 4.68
λ	0.86 - 1.85	0.86 - 1.85	0.86 - 1.85
α	0.85	0.85	0.85
k	0.029	0.029	0.029
H_i/s	2.50	9.58	16.67

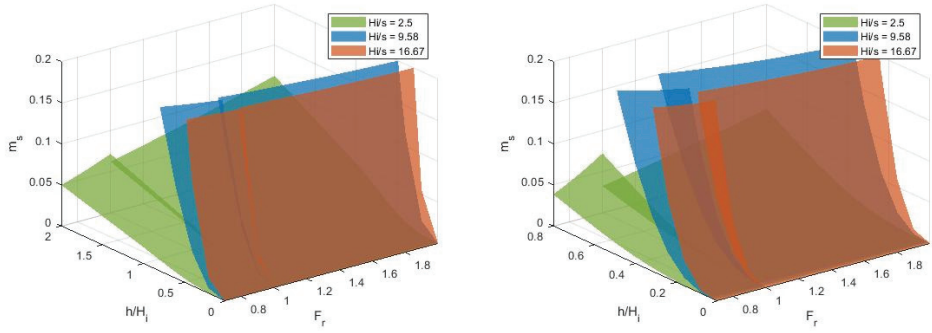

(a) (b)

Figure 9 - Effects of the geometrical vertical slenderness H_i/s parameter for b/w equal to 0.1 (a) and 0.6 (b)

The geometrical vertical slenderness of the masonry wall affects the vertical bending mechanisms activation, as expected. The vertical bending mechanism is a flexural mechanism and the activation is triggered when the external bending moment equals the flexural capacity of the cross-section, not depending on H_i/s. Therefore, slender elements (high value of H_i/s parameter) compared to squat elements are more vulnerable to flexural mechanisms. The friction block affects mainly the discontinuity of the surfaces while changing the flow regime.

In Figure 10, the effects of the numerical coefficient k are investigated and the values assumed for the main parameters are shown in Table 6.

Table 6 - Values of the parameters assumed to describe the maximum bending moment surfaces in Figure 10

Parameter	Maximum bending moment - Surface 1	Maximum bending moment - Surface 2	Maximum bending moment - Surface 3
b/w	0.6	0.6	0.6
C_D	4.68	4.68	4.68
λ	1.85	1.85	1.85
α	0.85	0.85	0.85
k	0.003	0.029	0.055
H_i/s	9.58	9.58	9.58

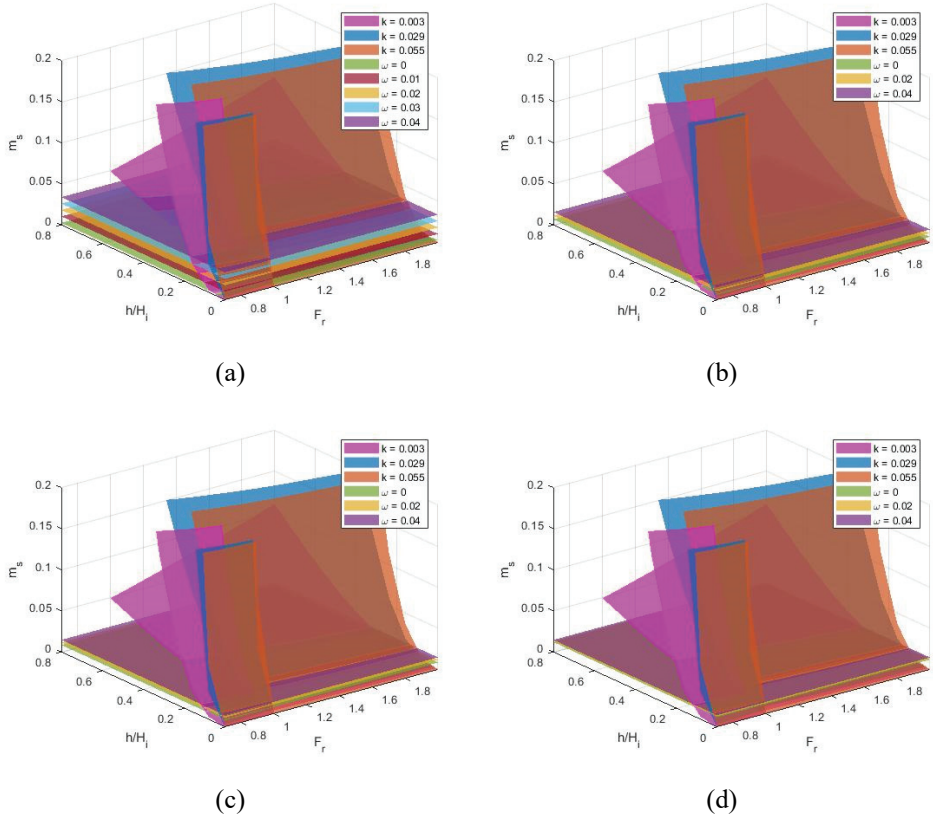

Figure 10 - Effects of the numerical coefficient k for n equal to 0.05 (a), 0.15 (b), 0.20 (c) and 0.35 (d)

The numerical coefficient k depends on the specific weight of water, γ_w, the interstorey height, H_i, and the compressive strength of masonry, f_m. The specific weight of water is approximately constant (effects of debris and sediment in the case of tsunami can be expected); the numerical coefficient k allows to investigate indirectly the effects of the interstorey height H_i. The vulnerability is high for high values of the k coefficient because the slenderness of the wall is increasing.

8. CONCLUSIONS

The main aim of this paper is to analyse the behaviour of masonry walls under tsunami loads in terms of out-of-plane (OOP) local mechanisms activation and the benefits of strengthening systems.

Strengthening systems with composite material represent an important innovation in the civil engineering techniques to retrofit existing buildings because it is not invasive on the structure, in terms of mass, stiffness and dynamic response, and it is recommended to preserve safety of cultural heritage in the case of FRCM or CRM where resin matrix is substituted by mortar.

The vertical bending mechanisms activation is investigated as main OOP local mechanism of the masonry wall under tsunami loads.

The tsunami load is modelled by the Foster et al. [12] model where the external loads are modelled by a hydrostatic plus a hydrodynamic load pattern.

Linear analyses are performed considering a simply supported beam as static model assuming a safety criterion to analyse the bending moment trend. In addition, an external axial load is modelled to simulate the wall self-weight and the effect of upper storeys due to the effects of the external axial load on the cross-section capacity.

Equations in dimensionless form are provided to describe the maximum external bending moment trend and the cross-section capacity in terms of bending moment in order to provide generalizable results applicable to any masonry wall cross-section and tsunami, but excluding masonry suffering for premature disaggregation.

Several parametric analyses are performed and the results are shown in terms of 3D charts in order to analyse the effects of the main parameters on the external bending moment trend and on the strengthening system. The inundation depth, the Froude number and the bending moment are shown on the axes. The inundation depth and the Froude number are the main parameters related to the hydrostatic and the hydrodynamic load.

The investigated main parameters are the external axial load n, the blocking fraction b/w, the wall openings coefficient, the vertical geometrical slenderness of the wall and the composite mechanical percentage.

Low composite mechanical values provide huge percentage effects in terms of bending moment capacity due to tensile behaviour added to unreinforced masonry cross-section, while benefits of high composite mechanical ratio could be negligible. This is due to the fact that increasing the external axial load, the effects of the strengthening systems are minimal due to the increasing of the neutral axis depth and consequentially, the lower strain of the composite.

The blocking fraction parameter has a high impact on the vulnerability of the masonry wall because it affects the flow regime and therefore, the external bending moment trend; the vulnerability of the masonry wall increases with the b/w coefficient. The wall openings have a high influence on the behaviour of masonry because the openings affect the load bearing area of the wall and the activation of the OOP local mechanism.

The geometrical vertical slenderness of the masonry wall affects the vertical bending mechanisms activation. In fact, the vertical bending mechanism is a flexural mechanism and the activation is triggered when the external bending moment equals the flexural capacity of the cross-section. Therefore, slender elements are more vulnerable to flexural mechanisms than squat elements.

Furthermore, the showed charts and the dimensionless equations are the bases of design tools for strengthening systems applied on masonry walls under tsunami loads to prevent the OOP vertical bending mechanism activation. The main parameters are the mechanical and geometrical parameters of masonry wall and composite system; safety factor has to be properly considered in the evaluation of the materials mechanical properties and external loads. In particular, it is important to balance properly such mechanical and geometrical parameters in order to design optimal strengthening systems, characterized by the best mechanical performance without economic waste.

Future work will take into account advanced constitutive behaviour of composites depending on specific assumed fiber and matrix. In addition, other local mechanisms will be taken into account as in-plane and out-of-plane local mechanisms in terms of bending and shear capacity.

Symbols

b = width of the structure;

b_m = width of the cross-section;

b/w = blocking fraction;

C_D = drag coefficient;

F_d = resultant of the hydrodynamic load distribution;

F_r = Froude number;

F_s = resultant of the hydrostatic load distribution;

f_f = tensile strength of strengthening system;

f_{fu} = ultimate tensile strength of strengthening system;

f_m = compressive strength of masonry;

g = gravitational acceleration constant;

E_f = elastic modulus of strengthening system;

E_m = elastic modulus of masonry;

k = numerical coefficient;

k_1 = numerical coefficient;

k_2 = numerical coefficient;

k_3 = numerical coefficient;

L = wall length;

$m_{s,1}$ = dimensionless bending moment equation for $h < H_i$;

$m_{s,2}$ = dimensionless bending moment equation for $h \geq H_i$;

$m_{R,0}$ = dimensionless ultimate bending moment of URM;

$m_{R,\omega}$ = dimensionless ultimate bending moment of strengthened cross-section;

n = dimensionless external axial load;

n_0 = dimensionless axial load of URM;

n_ω = dimensionless axial load of strengthened cross-section;

H_i = interstorey height;

h = expected inundation depth;

q_s = hydrostatic load;

q_d = hydrodynamic load;

s = thickness of masonry wall;

s/H_i = geometrical vertical slenderness of masonry wall;

t_f = equivalent thickness of fiber;

u = flow velocity;

w = channel width;

x = neutral axis depth;

α = opening ratio coefficient;

β = coefficient depending on the Froud number;

ε = generic strain;

ε_f = generic strain of strengthening system;

ε_m = generic strain of masonry;

ε_{m0} = peak strain of masonry;

ε_{mu} = ultimate strain of masonry;

ε_{fu} = ultimate strengthening system strain;

λ = empirical coefficient;

λ_m.= effective depth of compression zone centre of stress-block model;

γ_w = specific weight of water;

ψ_m = effective height of stress-block model;

ρ_s = flow density;

σ = generic strength;

ξ = dimensionless neutral axis depth;

ω = composite mechanical ratio.

References

[1] Strunz, G., Post, J., Zosseder, K., Wegscheider, T., et al. Tsunami risk assessment in Indonesia. Natural Hazards and Earth System Sciences, 11, 67-82, 2011. https://doi.org/10.5194/nhess-11-67-2011

[2] Behrens, J., Løvholt, F., Jalayer, F., et al. Probabilistic tsunami hazard and risk analysis: a review of research gaps. Frontiers in Earth Science, 9-114, 2021. http://doi.org/10.3389/feart.2021.628772

[3] Rafliana, I., Jalayer, F., Cerase, A., et al. Tsunami risk communication and management: Contemporary gaps and challenges. International Journal of Disaster Risk Reduction, 102771, 2022. http://doi.org/10.1016/j.ijdrr.2021.102771

[4] Athukorala, P.C., Resosudarmo, B.P. The Indian Ocean tsunami: Economic impact, disaster management, and lessons. Asian economic papers, 4(1), 1-39, 2005. https://doi.org/10.1162/asep.2005.4.1.1

[5] Palermo, D., Nistor, I., Saatcioglu, M., Ghobarah, A. Impact and damage to structures during the 27 February 2010 Chile tsunami. Canadian Journal of Civil Engineering, 40(8), 750-758, 2013. https://doi.org/10.1139/cjce-2012-0553

[6] Suppasri, A., Shuto, N., Imamura, F., et al. Lessons learned from the 2011 Great East Japan tsunami: Performance of tsunami countermeasures, coastal buildings, and tsunami evacuation in Japan. Pure and Applied Geophysics, 170(6-8), 993-1018, 2013. https://doi.org/10.1007/s00024-012-0511-7.

[7] Lorito, S., Behrens, J., Løvholt, F., et al. From Tsunami Science to Hazard and Risk Assessment: Methods and Models, Front. Earth Sci. 9:764922, 2021. https://doi.org/10.3389/feart.2021.764922.

[8] ASCE/SEI 7-22 Minimum Design Loads and Associated Criteria for Buildings and Other Structures, Reston, Virginia; 2021. https://doi.org/10.1061/9780784415788

[9] Fukuyama, H., Kato, H., Ishihara, T., et al. Structural design requirement on the tsunami evacuation buildings. US-Japan Cooperative Program in Natural Resources (UJNR), Tokyo; 2011.

[10] Asakura, R., Iwase, K., Ikeya, T., et al. An Experimental Study on Wave Force Acting on On-Shore Structures due to Overflowing Tsunamis. In Proceedings of Coastal Engineering Japan Society of Civil Engineers, Japan, 911-915, 2000.

[11] Okada, T., Sugano, T., Ishikawa, T., et al. Structural Design Method of Buildings for Tsunami Resistance. The Building Center of Japan, Japan, 2005

[12] Foster, A., Rossetto, T., Allsop, W. An experimentally validated approach for evaluating tsunami inundation forces on rectangular buildings. Coastal Engineering, 128, 44-57, 2017. https://doi.org/10.1016/j.coastaleng.2017.07.006

[13] Peiris, N., Pomonis, A. Decembre 26, 2004 Indian Ocean Tsunami: vulnerability functions for loss estimation in Sri Lanka. In Proceedings of the Geotechnical Engineering for Disaster Mitigation and Rehabilitation, Singapore, 2005.

[14] Mallawaarachchi, R.S., Jayasinghe, C. The effects of cyclones, tsunami and earthquakes on built environments and strategies for reduced damage. Journal of the National Science Foundation of Sri Lanka, 36, 03-14, 2008.

[15] Vlachakis, G., Cervera, M., Barbat, G. B., Saloustros, S. Out-of-plane seismic response and failure mechanism of masonry structures using finite elements with enhanced strain accuracy. Engineering Failure Analysis, 97, 534-555, 2019. https://doi.org/10.1016/j.engfailanal.2019.01.017

[16] Belliazzi, S., Lignola, G.P., Prota, A. Simplified approach to assess the vulnerability of masonry buildings under tsunami loads. Proceedings of the Institution of Civil Engineers-Structures and Buildings, 1-13, 2020. https://doi.org/10.1680/jstbu.20.00147

[17] Belliazzi, S., Lignola, G.P., Prota, A. Textile Reinforced Mortars systems: a sustainable way to retrofit structural masonry walls under tsunami loads. International Journal of Masonry Research and Innovation, 3(3), 200-222, 2018. https://doi.org/10.1504/IJMRI.2018.093484

[18] Ai, F., Comfort, L. K., Dong, Y., Znati, T. A dynamic decision support system based on geographical information and mobile social networks: A model for tsunami risk mitigation in Padang, Indonesia. Safety science, 90, 62-74, 2016. https://doi.org/10.1016/j.ssci.2015.09.022

[19] Fabbrocino, F., Belliazzi, S., Ramaglia, G., Lignola, G.P., Prota, A. Masonry walls retrofitted with natural fibers under tsunami loads. Materials and Structures, 54(3), 1-15, 2021. http://doi.org/10.1617/s11527-021-01707-9

[20] Belliazzi, S., Lignola, G.P., & Prota, A. Retrofit of Masonry Walls with Composites to Reduce Vulnerability to Tsunami Loads. In Proceedings of International Conference on Fibre-Reinforced Polymer (FRP) Composites in Civil Engineering, Istanbul, Turkey, 2021.

[21] Borri, A.; Corradi, M.; De Maria, A. The Failure of Masonry Walls by Disaggregation and the Masonry Quality Index. Heritage, 3, 1162-1198, 2020. https://doi.org/10.3390/heritage3040065

[22] Belliazzi, S., Lignola, G.P., Di Ludovico, M., Prota, A. Preliminary tsunami analytical fragility functions proposal for Italian coastal residential masonry buildings. Structures, 31, 68-79, 2021. https://doi.org/10.1016/j.istruc.2021.01.059

[23] Lloyd, T. O. An experimental investigation of tsunami forces on coastal structures (Doctoral dissertation, UCL (University College London)), 2016.

[24] Qi, Z.X., Eames, I., Johnson, E.R. Force acting on a square cylinder fixed in a free-surface channel flow. Journal of Fluid Mechanics, 756, 716-727, 2014. https://doi.org/10.1017/jfm.2014.455

[25] Eurocode 6 - Design of Masonry Structures; EN 1996. Design of Masonry Structures, part 1.1: General Rules for Reinforced and Unreinforced Masonry Structures, Brussels, Belgium. 2006.

[26] de Felice, G., Aiello, M.A., Caggegi, C., et al. Recommendation of RILEM Technical Committee 250-CSM: Test method for Textile Reinforced Mortar to substrate bond characterization. Materials and Structures, 51 (4), 95, 2018. https://doi.org/10.1617/s11527-018-1216-x

[27] CNR DT 200R1/2013 Guide for the Design and Construction of Externally Bonded FRP Systems for Strengthening Existing Structures, Rome, Italy. 2014.

[28] CNR DT 215/2018 Guide for the Design and Construction of Externally Bonded Fibre Reinforced Inorganic Matrix Systems for Strengthening Existing Structures, Rome, Italy. 2020.

[29] Zinno, A., Lignola, G.P., Prota, A., et al. Influence of free edge stress concentration on effectiveness of FRP confinement. Composites Part B: Engineering, 41(7), 523-532, 2010. https://doi.org/10.1016/j.compositesb.2010.07.003

[30] Belliazzi, S., Ramaglia, G., Lignola, G.P., Prota, A. Out-of-plane retrofit of masonry with fiber-reinforced polymer and fiber-reinforced cementitious matrix systems: normalized interaction diagrams and effects on mechanisms activation. Journal of Composites for Construction, 04020081, 25 (1), 2021. http://doi.org/10.1061/(ASCE)CC.1943-5614.0001093

[31] Priestley, M. J. N., Seible, F. Design of seismic retrofit measures for concrete and masonry structures. Construction and Building Materials, 9(6), 365-377, 1995. https://doi.org/10.1016/0950-0618(95)00049-6

[32] D'Ayala, D., Speranza, E. Definition of collapse mechanisms and seismic vulnerability of historic masonry buildings. Earthquake Spectra, 19(3), 479-509, 2003. https://doi.org/10.1193%2F1.1599896

[33] Milano, G., Lourenço, P., Tralli, A. Homogenization Approach for the Limit Analysis of Out-of-Plane Loaded Masonry Walls. Journal of Structural Engineering. 132 (10), 1650-1663, 2006. https://doi.org/10.1061/(ASCE)0733-9445(2006)132:10(1650)

[34] De Lorenzis, L. Strengthening of masonry structures with fibre-reinforced polymer (FRP) composites. Strengthening and Rehabilitation of Civil Infrastructures Using Fibre-Reinforced Polymer (FRP) Composites. Woodhead Publishing, eds Hollaway LC and Teng JG: 235-266, 2008. https://doi.org/10.1533/9781845694890.235

[35] Guadagnuolo, M., Faella, G. The friction in the out-of-plane failure mechanisms of masonry walls. In: Proceedings of the 14th International Brick and Block Masonry Conference. Sydney: Cracow University of Technology, Silesian University of Technology and Wroclaw University of Technology, 2008

[36] D'Altri, A. M., De Miranda, S., Castellazzi, G., Sarhosis, V. A 3D detailed micro-model for the in-plane and out-of-plane numerical analysis of masonry panels. Computers and Structures, 18-30, 206, 2016. https://doi.org/10.1016/j.compstruc.2018.06.007

[37] Harish, S., Sriram, V., Schüttrumpf, H., Sannasiraj, S. A. Tsunami-like flow induced forces on the structure: Dependence of the hydrodynamic force coefficients on Froude number and flow channel width in quasi-steady flow phase. Coastal Engineering, 168, 103938, 2021. https://doi.org/10.1016/j.coastaleng.2021.103938

[38] D'Antino, T., Calabrese, A. S., Poggi, C. Experimental procedures for the mechanical characterization of composite reinforced mortar (CRM) systems for retrofitting of masonry structures. Materials and Structures, 53(4), 1-18, 2020. https://doi.org/10.1617/s11527-020-01529-1

[39] de Santis, S., de Felice, G., Di Noia, G. L., Meriggi, P., Volpe, M. Shake table tests on a masonry structure retrofitted with composite reinforced mortar. Key Engineering Materials, 817, 342-349, 2019. https://doi.org/10.4028/www.scientific.net/KEM.817.342